Int. J. Electron. Commun. (AEÜ) 93 (2018) 123–131

Contents lists available at ScienceDirect

Int. J. Electron. Commun. (AEÜ)

journal homepage: www.elsevier.com/locate/aeue

Regular paper

# A dual polarized multiband rectenna for RF energy harvesting

Neeta Singh[a], Binod K. Kanaujia[b,*], Mirza Tariq Beg[a], Mainuddin[a], Taimoor Khan[c], Sachin Kumar[d]

[a] Department of Electronics and Communication Engineering, Jamia Millia Islamia, New Delhi 110025, India
[b] School of Computational and Integrative Sciences, Jawaharlal Nehru University, New Delhi 110067, India
[c] Department of Electronics and Communication Engineering, National Institute of Technology, Silchar 788010, India
[d] Department of Electronics & Communication Engineering, SRM Institute of Science and Technology, Chennai, Tamil Nadu 603203, India

ARTICLE INFO

*Keywords:*
Circular polarization
Energy harvesting
Multiband
Rectenna

ABSTRACT

The paper presents a multiband dual polarized rectenna for RF energy harvesting in C-band application range. The receiving antenna of the designed rectenna is consisting of a truncated corner square patch loaded with several circular slots, L-slots and U-slot. A proximity coupled feeding arrangement is used for obtaining a wide impedance bandwidth so that the complete C-band from 4 to 8 GHz can be covered. The proposed antenna has the advantage of compact size and dual polarization since circular polarization is realized at three bands (5.42 GHz, 6.9 GHz and 7.61 GHz) in the −10 dB impedance bandwidth range. For efficient RF to DC conversion a two-stage voltage doubler rectifier is used considering that it provides a higher voltage multiplication with a small threshold voltage at its primary stage. For ensuring maximum RF to DC conversion efficiency; a matching network has been designed and is connected in between receiving antenna and the rectifier circuitry in order to match the antenna and load in different frequency bands. It is observed that a maximum conversion efficiency of 84% is achieved at 5.76 GHz. The proposed rectenna has been fabricated and it is found that measured results are in good match with the simulated results.

## 1. Introduction

In the recent time, there is a huge demand for portable wireless devices operating in L, S and C application bands. Due to the increasing demand for wireless equipment in every aspect of day to day life, RF energy harvesting can be a suitable and viable solution for replacing batteries in portable handheld devices. The idea of RF energy harvesting was proposed in the 20th century and involves the conversion of electromagnetic waves present in surrounding to direct current (DC) electricity [1]. During the last few years, a number of methods for harnessing energy from the surrounding (heat, light, pressure, motion, RF/microwave signals) or other energy sources such as human body (foot strike, finger strokes, body heat) have been proposed [2,3]. Among the different techniques proposed, the method using rectenna technology to convert ambient RF to DC power is much popular because this method promises a vast scope by providing an alternative green energy solution to low power electronics and electrical devices. The rectenna or rectifying antenna is basically comprised of an antenna element, a low pass filter, impedance matching circuitry, rectifier and a DC pass filter [4]. In this system, the energy of time-varying electromagnetic waves is sensed by an antenna which is integrated with a rectifier by means of an impedance matching network and low pass filter. The DC filter blocks the higher order harmonics generated by non-linear rectifying diodes. The major limitation of ambient RF wireless energy harvesting system is the small RF to direct current conversion efficiency as low RF energy is present in the environment.

Over the last two decades, various designs of receiving antenna and rectifier have been proposed by a number of researchers [5–14]. A two diode rectenna with a coplanar strip line fed antenna element is proposed in [5]. The rectenna is reported for 5.8 GHz frequency band with rectennas interconnected in series, parallel and cascaded configuration to form the rectenna array. A rectenna with omnidirectional and linear polarization radiation characteristics is proposed for mobile applications [6]. The proposed design is comparatively compact in size by using a fractal Koch antenna geometry. In reference [7], a rectenna with dual band antenna has been presented. A tradeoff between proposed rectenna size and received power is shown in the literature and it is demonstrated that the design operates better in the GSM 1800 and UMTS 2100 cellular bands. Another rectenna design with a triple band and a dual port has been shown in [8]. The design employs two stacked antennas with L-probe feeding to cover a large bandwidth; the design operates for GSM 900, GSM 1800 and UMTS 2100 mobile

* Corresponding author.
*E-mail addresses:* bkkanaujia@yahoo.co.in (B.K. Kanaujia), mtbeg@jmi.ac.in (M.T. Beg), mainuddin@jmi.ac.in (Mainuddin).

https://doi.org/10.1016/j.aeue.2018.06.020
Received 16 February 2018; Accepted 9 June 2018

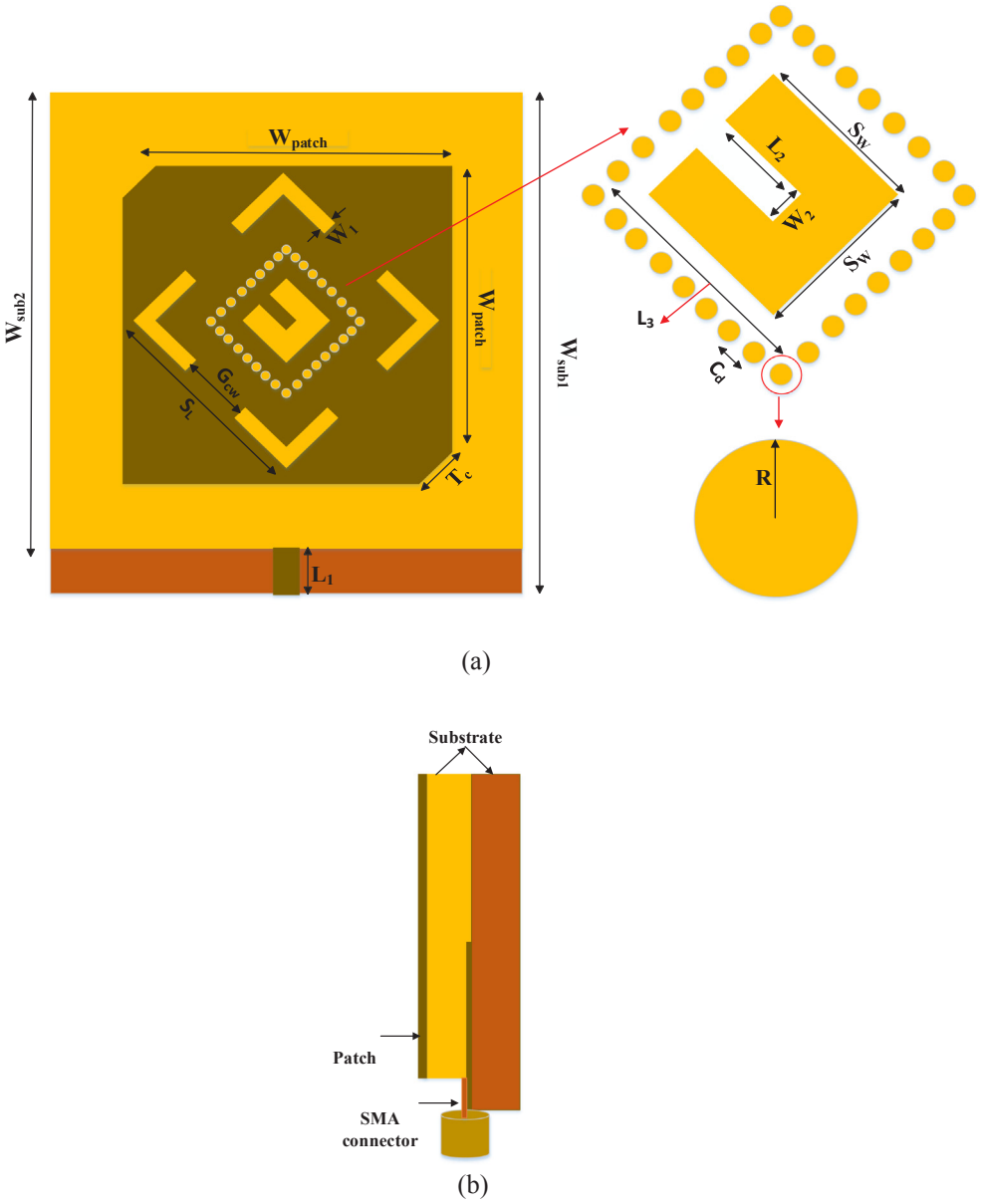


**Fig. 1.** Layout of the proposed antenna design (a) top view (b) side view.

communication bands. A quad band rectenna with stacked design has been reported in reference [9]. The RF-to-DC conversion efficiency of presented design is almost double compared to single tone rectenna. A tetra band rectenna for Wi-Fi and GSM wireless bands is reported in the reference [10]; the proposed tetra band rectenna results have been validated by the help of genetic algorithm based optimizations.

An antenna plays a crucial role in maximizing RF-to-DC conversion efficiency. The receiving antenna operating frequency, bandwidth, gain, efficiency and radiation characteristic decides the amount of energy handled by the rectifying circuit of the rectenna. The antenna is the main sensing element which directly participates in the conversion process of RF to DC power; therefore, its role is of much importance. A number of antenna structures have been proposed by various researchers such as with single [11], dual [12,13] and multiple [14] radiating bands for sensing electromagnetic waves. A compact asymmetric coplanar strip fed and capacitance terminated antenna for dual band WLAN applications is presented in [15]. An antenna with meandered monopole radiator for dual band characteristics is proposed in [16], the antenna resonances can be controlled by adjusting the dimensions of the meandered monopole. In [17], an antenna with triple band notching and reconfigurable characteristics is presented for cognitive radio applications. A microstrip line fed inverted U-shaped patch antenna having partial ground plane integrated with a toothbrush shaped strip and meandered line strip is reported for triple band WLAN and WiMAX applications [18]. An antenna making use of stepped impedance stub loaded stepped impedance resonators for achieving multiple radiating bands is presented in [19]. An antenna using composite right/left handed transmission line array has been reported for multiple resonant modes [20], the proposed antenna has a small frequency ratio value between the resonating bands. A leaky wave metamaterial antenna consisting of complementary split ring resonators and capacitive gaps is presented for omnidirectional radiation behaviour [21]. An antenna based on multi-layered fractal perturbed mushrooms is presented in [22]; the presented antenna structure suppresses the effect of cross polarization radiations significantly. A dual band chiral metamaterial inspired by the fractal concept is proposed in [23]; the reported polarizer can be easily integrated with other devices. The paper [24] presents three circularly polarized patch antennas with combined meta-surfaces and meta-resonators; the antennas have the advantage of miniaturized antenna size, wide bandwidth and good radiation

efficiency. However, a single or dual band antenna is not of much use because the conversion of ambient RF energy is low in the case of a single or double band; hence output power generated will be low. An array can be used to obtain a sufficient amount of power level but this type of rectenna configurations are difficult to realize and fabricate and occupies more space as well. A triple band or quad band system may be a better idea to increase the level of power, but multiple antenna ports and fractal antenna geometry increases the design complexity. In addition, most of the reported receiving antennas operate only for linearly polarized waves; however, for modern wireless applications circularly polarized waves are to be radiated. More, the difficulty of orientation mismatch between transceivers in wireless reception can be solved by making use of circularly polarized antennas. Therefore, there is a need of compact, multiband, dual polarized rectenna for ambient RF energy harvesting system.

In this communication, a dual polarized multiband rectenna for ambient RF energy harvesting is proposed in support of C-band frequency range applications. The designed rectifier system is consisting of a microstrip patch antenna working for six application bands (4.75 GHz, 5.42 GHz, 5.76 GHz, 6.4 GHz, 6.9 GHz and 7.61 GHz) in the range of 4–8 GHz. The proposed antenna has the advantage of compact size and dual polarization as circular polarization is realized at frequencies 5.42 GHz, 6.9 GHz and 7.61 GHz. A RF matching network is designed to match 50 Ω impedance of the antenna with the impedance of rectifier. For the purpose of rectification, a two-stage voltage doubler rectifier is used since it provides a higher voltage multiplication with a small threshold voltage at its initial stage. A conversion efficiency of 84% is achieved at frequency 5.76 GHz with 15 dBm input power level. For the simulation and development of proposed antenna, Finite Element Method (FEM) based commercially available tool Ansys HFSS is used and simulations related to the rectifier and matching circuitry are conducted using Keysight ADS. A prototype rectenna has been fabricated and found simulated and measured results are in good agreement. The paper is organized into three sections with Section 2 explaining the design of microstrip patch antenna. A multiband rectifier, matching network and non-linear behaviour of the diode is analyzed in Section 3 followed by a brief conclusion in Section 4.

## 2. Antenna geometry

The schematic of proposed patch antenna is illustrated in Fig. 1. The antenna structure is consisting of a square patch loaded with several slots, ground surface and proximity coupled feeding arrangement. This type of feed technique is also called as the electromagnetic coupling scheme. As shown in Fig. 1, the two dielectric substrates are used in such a manner that the feed line is present in between the two substrates. The radiating patch and ground plane are present on the top and bottom of the upper substrate and lower substrate, respectively. The main advantage of proximity coupled feed technique is that it eliminates spurious feed radiations and provides a very wide impedance bandwidth, due to the overall increase in thickness of the microstrip patch antenna. By controlling the length of the feed line and the width to line ratio of the patch, the impedance matching can be achieved.

The antenna design lies in five steps as shown in Fig. 2. By loading the patch with rotated U-slot of suitable dimensions bandwidth enhancement can be realized in the designed structure. The currents along the edges of loaded U-slot introduce additional resonances, which in addition to the resonance of the main square patch, produce an overall wideband radiation characteristic. The U-slot introduces a capacitive reactance which counteracts the inductive reactance of the probe leading to a wideband performance. Further, the loaded small circular shaped slots play a significant part in achieving multiband characteristics; due to the capacitive loading of the square radiating patch several notch bands can be achieved within the antenna impedance bandwidth. The circular shaped slots of radius $R$ are loaded in such a fashion that it forms a diamond-like ring around the rotated U-slot. It has been found that by loading the antenna with rotated U-slot and several circular shaped slots, the antenna achieves wide bandwidth with multiple resonating bands. More, the antenna corners are truncated by means of a right-angled isosceles triangle for generating orthogonal current modes of almost same amplitude and with 90-degree phase difference between them to excite circularly polarized band. Similarly, two pairs of rotated L-shaped slots are used for the excitation of circularly polarized bands and improving the return loss bandwidth of the antenna. The amount of axial ratio bandwidth can be varied by altering the dimensions of the arms of L-slots. FR-4 substrate with relative permittivity 4.4, loss tangent 0.02 and thickness 0.8 mm is considered for designing the antenna structure. The proximity coupled feeding provides a choice between two different dielectric substrates, one for the feed line and other for the radiator. But here for this study, the same substrate is used for designing the antenna feed and radiating element. The fabricated antenna prototype is shown in Fig. 3. The total size of the upper substrate and lower substrate are $40 \times 40 \times 0.8\,mm^3$ and $40 \times 45 \times 0.8\,mm^3$ respectively. The effective specifications of the designed antenna are shown in Table 1.

### 2.1. Antenna measurement

Fig. 4(a) presents the variation of reflection coefficient ($S_{11} < -10$ dB) with frequency for an ordinary square patch (Step-1), square patch with U-slot (Step-2) and antenna with loaded circular slots and U-slot in the square patch (Step-3). Firstly, a simple square patch with proximity coupled feed is made to occupy a wide frequency range; compared to the conventional square patch which has a narrow bandwidth. Then, a rotated U-slot and circular slots are loaded in the radiating surface for converting a wide bandwidth (of 4–8 GHz) into multiple band radiation characteristics. The radius of loaded circular slots and dimensions of U-slot can be varied and optimized according to the application band required. Fig. 4(b) presents the variation of axial ratio with frequency for the proposed multiband antenna (Step-4). The designed microstrip patch antenna radiates six application bands in the range of 4–8 GHz. At three frequencies (5.42 GHz, 6.9 GHz and 7.61 GHz), the antenna radiates circularly polarized wave whereas for other three frequencies (4.75 GHz, 5.76 GHz and 6.4 GHz), the antenna shows linear polarization behaviour. The electrical characteristic of the fabricated antenna structure is measured by VNA of model N5230A Agilent PNA L series. The measured and simulated $S_{11}$ variation with frequency for the proposed antenna is shown in Fig. 5. As can be observed from Fig. 5, the proposed antenna resonates for six frequency bands 4.75 GHz (4.55–4.85 GHz), 5.42 GHz (5.25–5.5 GHz), 5.76 GHz (5.6–5.85 GHz), 6.4 GHz (6.25–6.5 GHz), 6.9 GHz (6.8–7 GHz) and 7.61 GHz (7.5–7.75 GHz) in the 4–8 GHz range. The simulated and measured $S_{11}$ are in a good agreement. A small deviation in measured and simulated results is seen which is due to photolithography fabrication process and soldering of SMA connector.

Fig. 6 represents the measured and simulated axial ratio comparison of the proposed antenna in the preferred band range. For optimizing the results of antenna and showing axial ratio variation, slots of different shapes and sizes are loaded at the centre and corner of the patch. The antenna shows circular polarization in the three resonating bands 5.42 GHz, 6.9 GHz and 7.61 GHz. The circular polarization (at 5.42 GHz) is achieved by means of truncated corners of the square microstrip patch. More, when two pairs of rotated L-slots are embedded into the square patch, the antenna excites circularly polarized waves in the two bands (6.9 GHz and 7.61 GHz). The simulated and measured gain of the designed antenna is given in Fig. 7. A peak gain of around 7.4 dBi is observed within the resonating impedance band. Fig. 8 shows the simulated surface current distribution of the proposed antenna in all the six resonating bands.

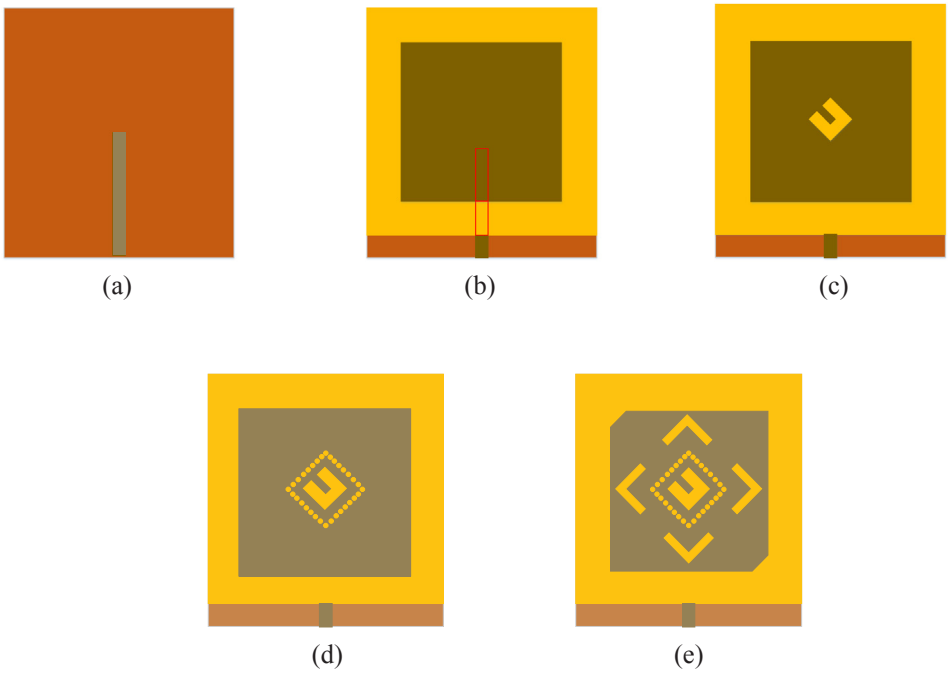


**Fig. 2.** Schematic of the antenna designing steps (a) Step-0 (b) Step-1 (c) Step-2 (d) Step-3 (e) Step-4.

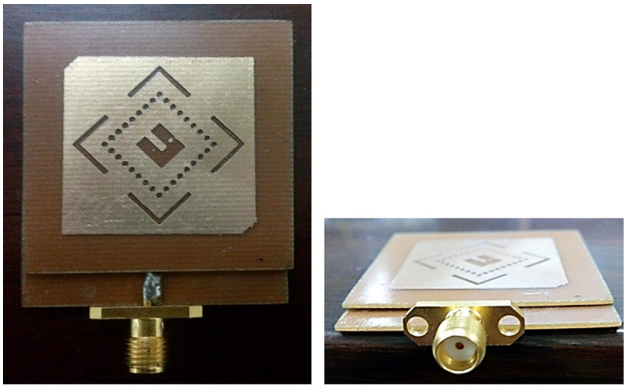


**Fig. 3.** Fabricated antenna prototype (a) top view (b) side view.

**Table 1**
Dimension of the proposed antenna.

| Parameters | (mm) |
|---|---|
| $W_{sub1}$ | 45 |
| $W_{sub2}$ | 40 |
| $W_{patch}$ | 26 |
| $S_L$ | 18 |
| $S_W$ | 5.5 |
| $G_{cw}$ | 4.5 |
| $T_c$ | 2.82 |
| $L_1$ | 19.1 |
| $W_1$ | 0.8 |
| $L_2$ | 3.5 |
| $W_2$ | 1 |
| $L_3$ | 10 |
| $R$ | 0.5 |
| $C_d$ | 1 |

## 3. Multiband rectifier

The RF signal sensed by the proposed patch antenna is an alternating current (AC) signal and in order to obtain a DC power, rectification of the RF signal is required. It is much desire to have a rectifier circuit with low power consumption and high power handling capability. For the present study, a two-stage voltage doubler rectifying circuit (Fig. 9(a)) is used since it provides a higher voltage multiplication with a small threshold voltage at its primary stage. However, there is a tradeoff between the number of stages and sensitivity and efficiency of the rectifier. It can be seen that as the number of stages in a multiplier increases, the loss at each stage also increases but with a higher multiplication factor and lower threshold voltage. However, in the case of fewer stages, a voltage drop will be small but needed a higher threshold value for all stages to work concurrently. Thus, a voltage multiplier turns out to be more sensitive when stages are more while it becomes more efficient when the stages are less.

In the two-stage voltage doubler rectifying circuit shown in Fig. 9(a), zero biased Schottky diodes HSMS 2820 are used for the rectification of RF signal. The Schottky diode is prefered due to its fast switching time, high current density, low threshold voltage and high efficiency. The harmonic balance method in ADS is considered as a good option when dealing with non-linear circuits in the frequency domain to ensure higher efficiency and better return loss characteristics.

A RF matching network is used to match the 50 Ω antenna impedance with the impedance of rectifier circuit. As the impedance of the antenna is frequency dependent, therefore it would be convenient to match it at single frequency rather than covering the whole frequency band at a time. Let the RF power signal received by the antenna and transferred to the rectifier can be expressed as $V_{IN} = V_c sin\omega t$, where $V_c$ is the amplitude of the signal and $\omega$ is the angular frequency of the wave. The topology of voltage doubler used in the design is shown in Fig. 9(a). During the positive half cycle, the diode $D_1$ is ON and $D_2$ is OFF; the wave is rectified by the help of series diode $D_1$ with rectified energy stored in capacitor$C_j$. For the negative half cycle, the diode $D_2$ is ON and $D_1$ is OFF; the wave is rectified by shunt diode $D_2$ and the rectified energy is stored in capacitor$C_i$. The value of capacitors $C_i$ and $C_j$ considered is 100 nF. The capacitor stores the energy thereby smoothening

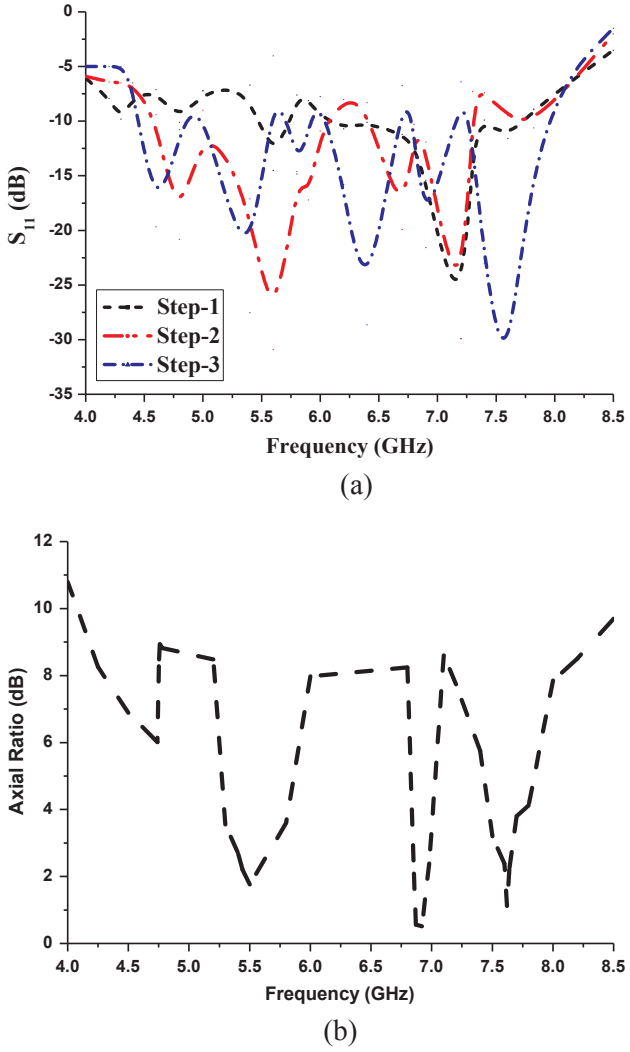


**Fig. 4.** Simulated results of the antenna designing steps (a) $S_{11}$ (b) axial ratio.

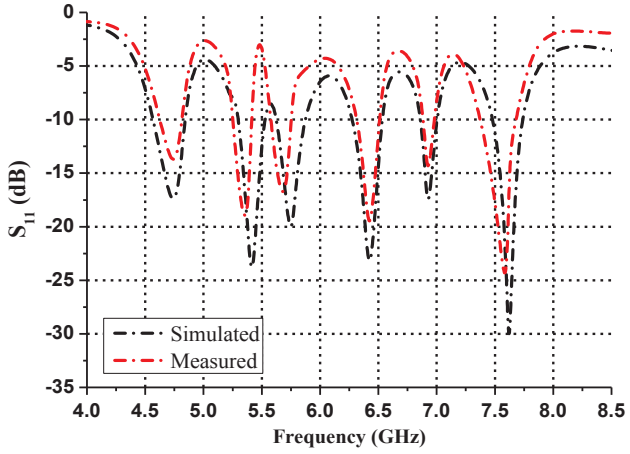


**Fig. 5.** Comparison of simulated and measured $S_{11}$ of the proposed antenna.

the DC output. The output DC voltage can be calculated by

$$V_{DC} = 2(V_c sin\omega t - V_{fr}) \quad (1)$$

where $V_{fr}$ is the diode forward bias voltage. The output DC voltge is evaluated as

$$V_{DC} = I_{DC} \times R_L \quad (2)$$

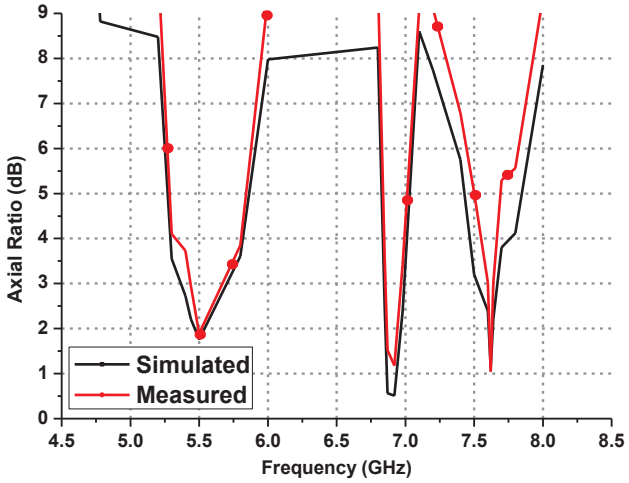


**Fig. 6.** Simulated and measured axial ratio of the proposed antenna.

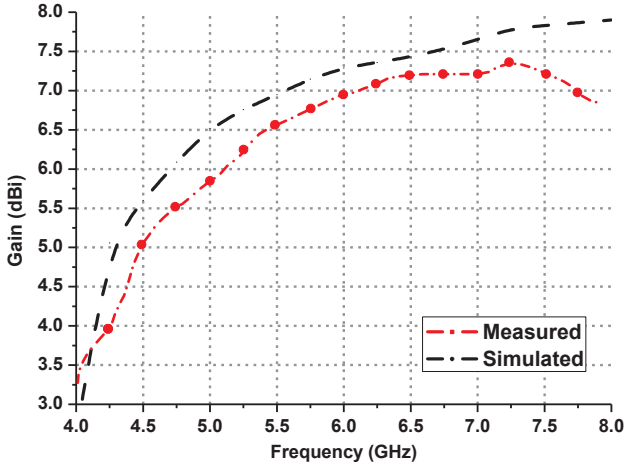


**Fig. 7.** Simulated and measured gain of the proposed antenna.

where $I_{DC}$is the output DC current and $R_L$ is the load resistance. The rectifier design parameters are given in Table 2. In the table, $W_{TL}$ is the width of transmission line and $L_{TL}$ is the length of transmission line. The parameter $W$, $L$ and $B$ represents width, length and angle of the radial stub respectively. $R_L$ is optimized as 3 KΩ for the given analysis.

### 3.1. Matching circuit

It is an important part of the rectenna circuit as matching circuit ensures maximum RF to DC conversion efficiency. The matching circuit shown in Fig. 9(b) is placed at the input of rectifier and output of the microstrip antenna. With the help of maximum power transfer theorem the matching can be understood; when source impedance and load impedance are complex conjugates of each other a maximum power is delivered to the load. In Fig. 10(a), the layout of proposed six band rectifier is shown. It can be seen from the figure that the rectifier has three branches with each branch consisting of an individual cell. Each cell present in the designed rectifier circuit operates for two resonating frequencies and further connected to a voltage doubler circuit. Therefore, this type of designed rectifier will act as a triple voltage doubler circuit consequently increasing the output voltage. Fig. 10(b) represents the fabricated prototype of the multiband rectifier. FR-4 substrate with dielectric constant 4.4 and thickness 0.8 mm is used for the fabrication of rectifier and the overall size of PCB is 90 × 100 $mm^2$.

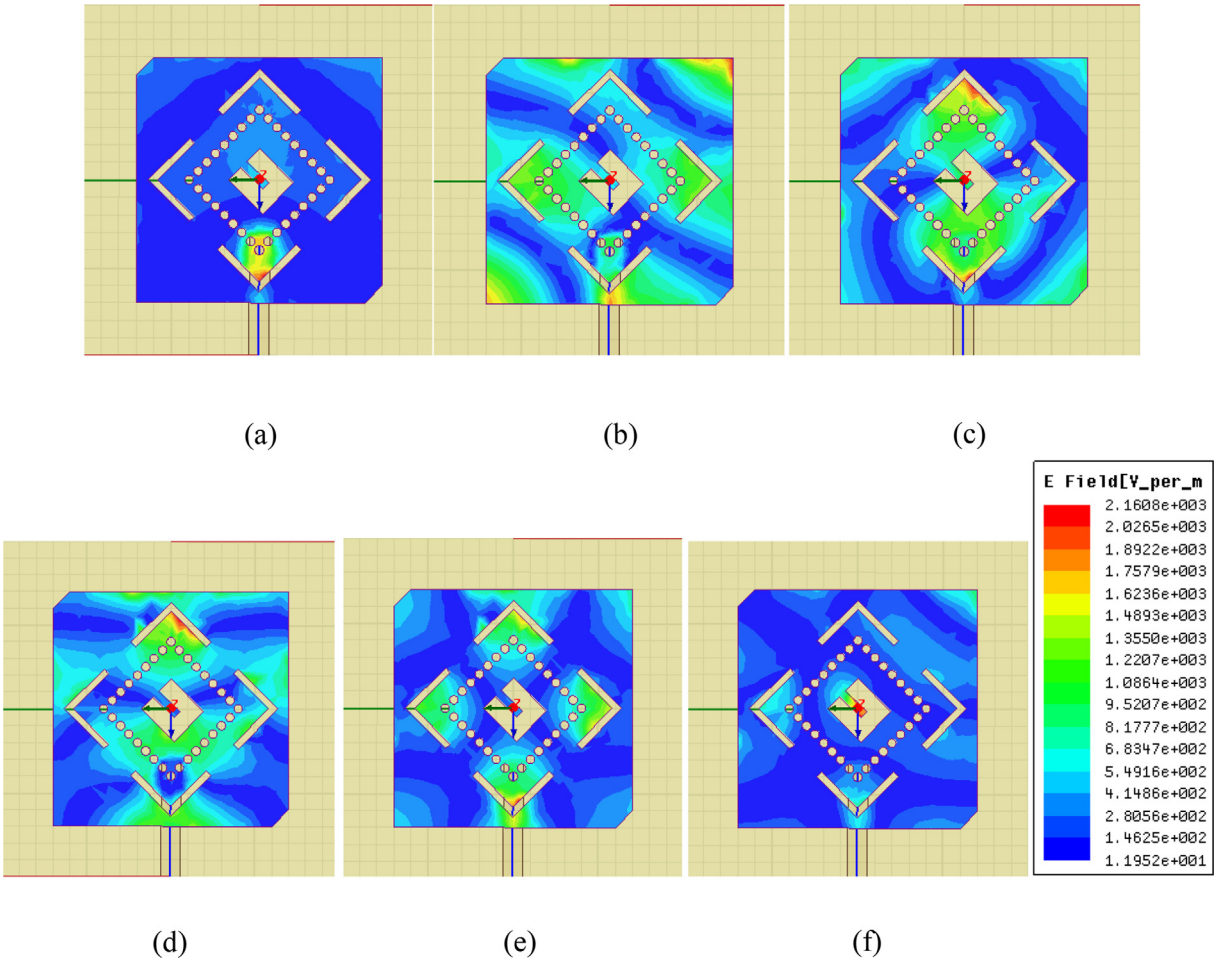


**Fig. 8.** Simulated surface current distribution of the designed antenna (a) 4.75 GHz (b) 5.42 GHz (c) 5.76 GHz (d) 6.4 GHz (e) 6.9 GHz (f) 7.61 GHz.

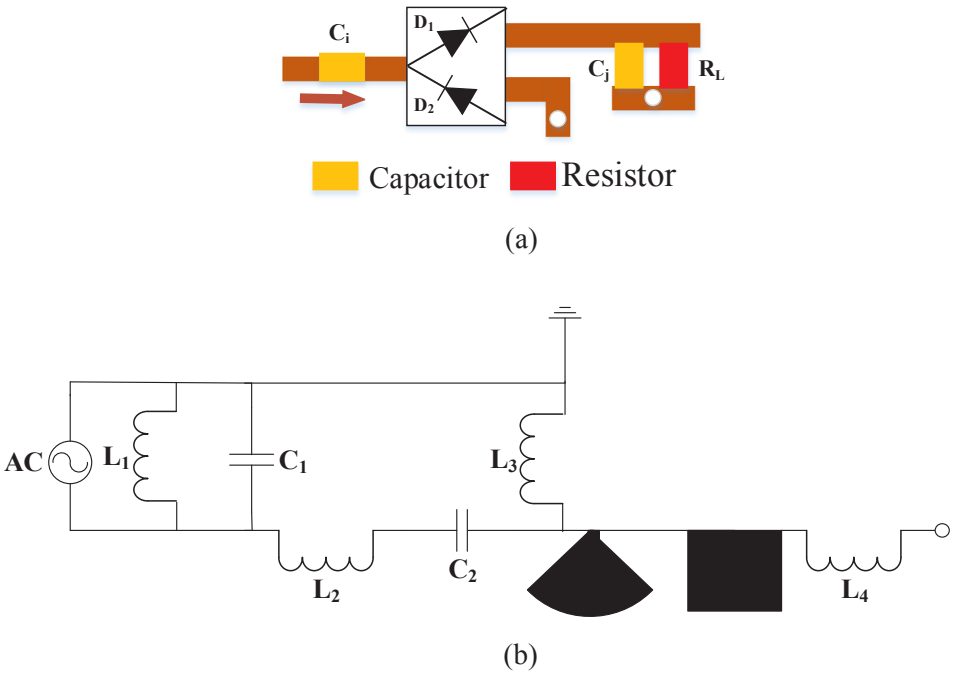


**Fig. 9.** Layout of the proposed six band rectifier (a) voltage doubler rectifier circuit (b) impedance matching network.

**Table 2**
Design parameters of the rectifier.

| Parameters | Cell 1 | Cell 2 | Cell 3 |
|---|---|---|---|
| $L_1$ | 8.7 nH | 8.7 nH | 8.7 nH |
| $C_1$ | 1 pF | 0.513 pF | 0.400 pF |
| $L_2$ | 630 pH | 724 nH | 857 pH |
| $C_2$ | 2000 pF | 2000 pF | 100 nF |
| $L_3$ | 0.04 nH | 8.7 nH | 1 nH |
| $L_4$ | 1.47 nH | 1.6 nH | 2.069 nH |
| $W_{TL}$ | 65.9 mm | 29.06 mm | 22 mm |
| $L_{TL}$ | 21 mm | 23.92 mm | 25.59 mm |
| $W$ | 6113 mm | 1410 mm | 3.735 mm |
| $L$ | 18.51 mm | 0.759 mm | 14.14 mm |
| $B$ | 100° | 135° | 12.1° |

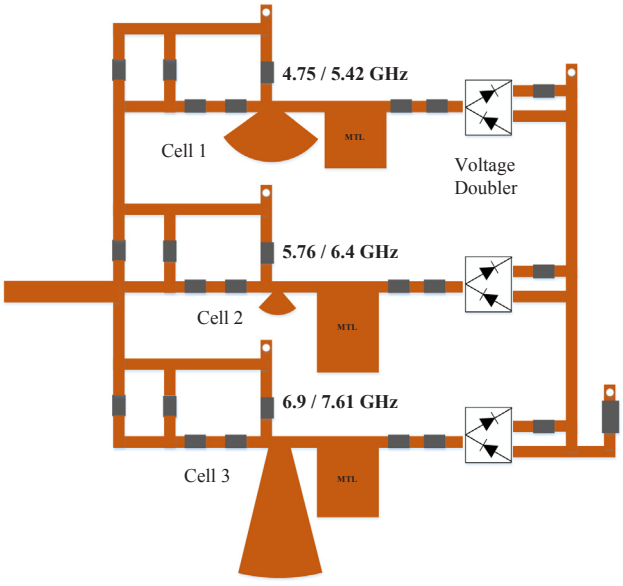


(a)

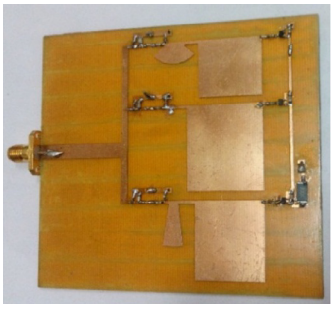

(b)

**Fig. 10.** Layout of the proposed six band rectifier (a) topology (b) fabricated prototype.

### 3.2. Rectenna measurement

For measuring the rectenna performance parameters, an SMA connector of 50 Ω is integrated with the rectifier. The overall efficiency of rectenna system depends upon the performance of the rectifier and receiving antenna and that of the quality of matching between the antenna and rectifier structure. The converted DC power in rectenna can be measured by the help of multimeter placed across the load resistance $R_L$. Fig. 11(a) and (b) illustrates the variation of output DC voltage with the input power level for frequency bands 4.75 GHz, 5.42 GHz, 5.76 GHz and 6.4 GHz, 6.9 GHz, 7.61 GHz respectively. From the figure, it can be seen that the simulated and measured output voltage are in match. A little difference in measured and simulated results

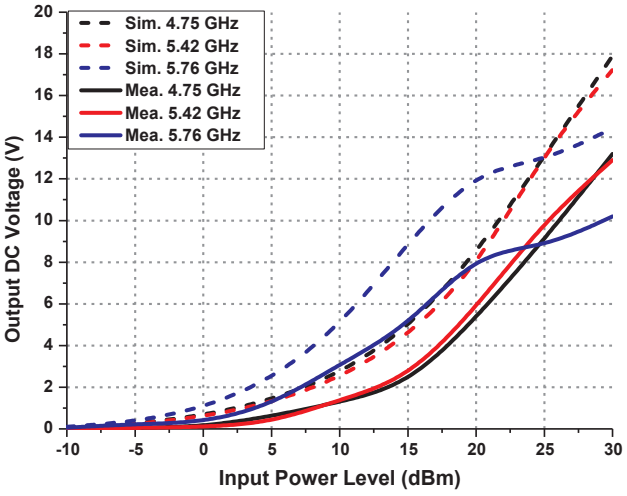


(a)

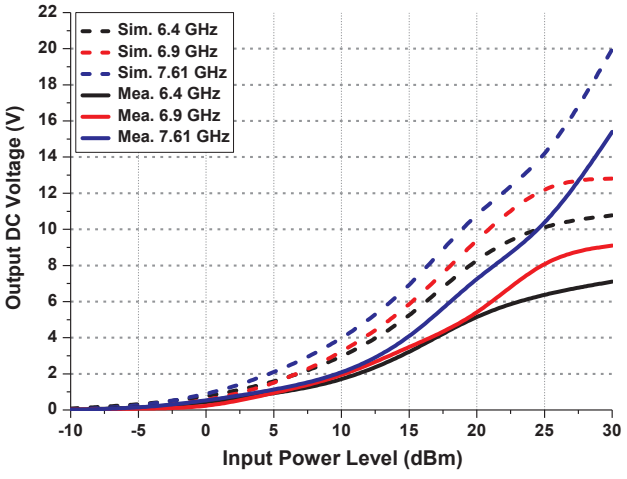


(b)

**Fig. 11.** Simulated and measured comparison of output DC voltage at frequency (a) 4.75 GHz, 5.42 GHz, 5.76 GHz (b) 6.4 GHz, 6.9 GHz, 7.61 GHz.

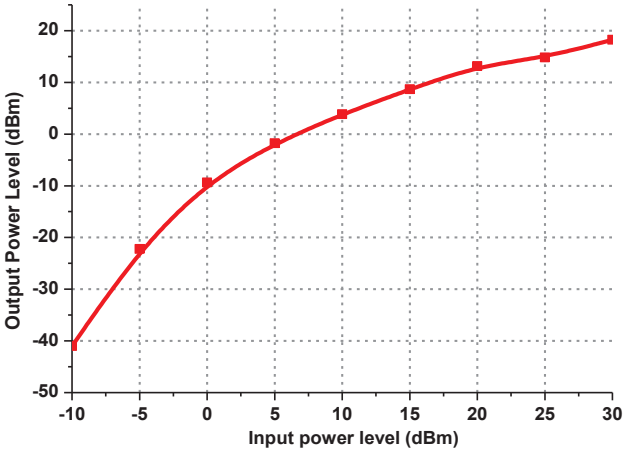


**Fig. 12.** Variation of output power with input power level.

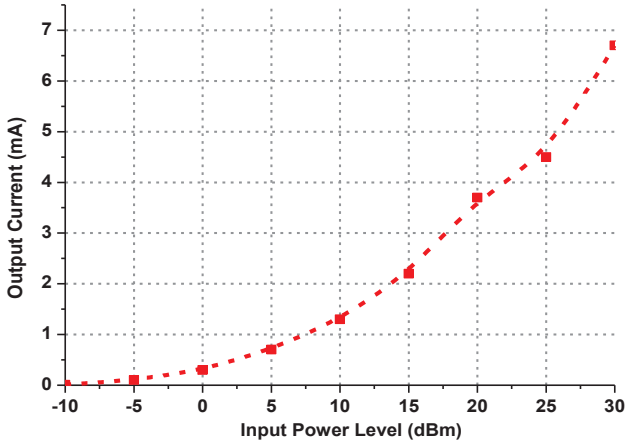


**Fig. 13.** Variation of output current with input power level.

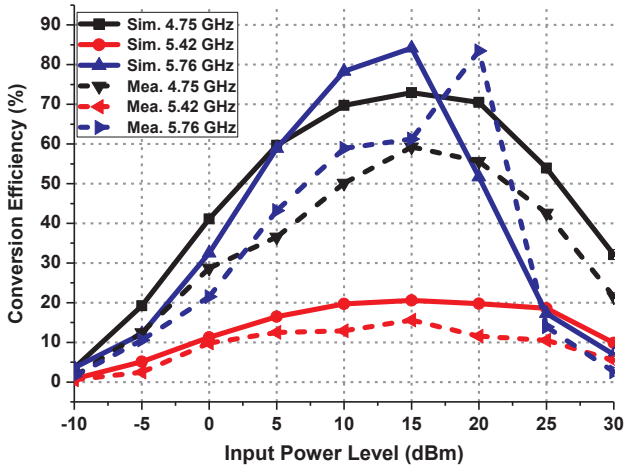


**Fig. 14.** Simulated and measured RF to DC conversion efficiency at frequency (a) 4.75 GHz, 5.42 GHz, 5.76 GHz (b) 6.4 GHz, 6.9 GHz, 7.61 GHz.

is seen due to the customary fabrication process and SMA connector soldering. Figs. 12 and 13 represent the variation of output power and output current with input power level, respectively. To protect the diode from a breakdown, a low input power level is maintained in both simulated and measured results.

A standard high gain horn antenna is used for evaluating the

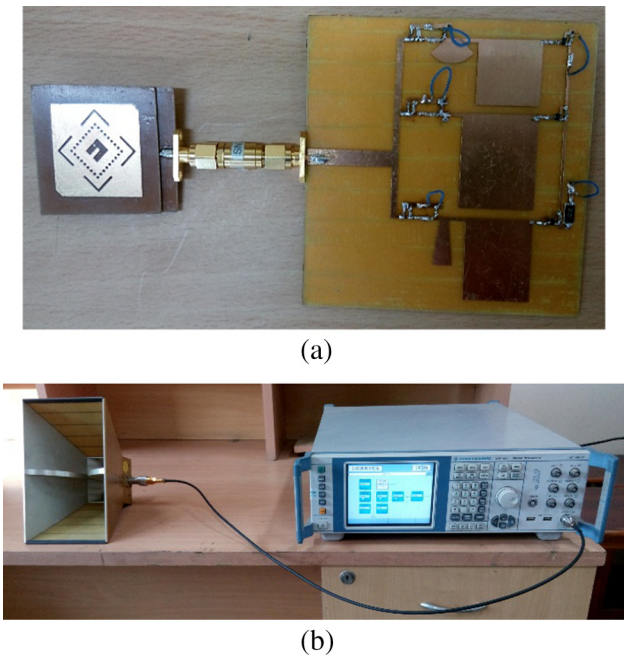


**Fig. 15.** (a) Fabricated prototype of the proposed antenna and rectifier (b) measurement setup.

performance of proposed rectenna. The transmitting horn antenna is connected to RF signal generator for generating an input power of 4–8 GHz. At the other end, a receiving horn antenna is connected with the spectrum analyzer to receive the signals radiated from opposite end. Further, the receiving horn antenna is replaced by the proposed rectenna and rectenna parameters can be calculated by the help of Friis transmission equation

$$P_r = \left(\frac{\lambda}{4\pi r}\right)^2 P_t G_t G_r \tag{3}$$

where $P_t$, $G_t$, $G_r$, $r$, and $\lambda$ are the transmitting power, gain of the transmitting and receiving antenna, distance between the two antennas and wavelength respectively. More, the input power is generated by the help of signal generator and the output DC value is measured via spectrum analyzer. The received power at the load can be calculated by [6]

$$\eta_{CE}\% = \frac{P_{DC}}{P_{in}} \times 100\% = \frac{V^2{}_{DC}}{R_L P_{in}} \times 100\% \tag{4}$$

$V_{DC}$ is the measured output DC voltage and $R_L$is the load resistance at the output. The conversion efficiency calculated using Eq. (4) is plotted in Fig. 14(a) and (b). Fig. 14 shows the simulated and measured conversion efficiency for all the six resonating bands. The efficiency of the proposed rectenna is not equal for all the six operating frequency bands. A low efficiency is obtained in many operating bands due to the lower value of the antenna efficiency at the corresponding frequency and also due to poor impedance matching between the antenna and rectifier at the concerned frequency. A maximum RF to DC conversion efficiency of 84% is achieved at 5.76 GHz for 15 dBm input power. As the efficiency in the current position is mostly limited due to the small input RF power, the actual efficiency can be further improved if more RF power is available at the receiving antenna. Fig. 15 illustrates the measurement setup and fabricated prototype of the proposed rectenna configuration. A comparison of proposed work with other reported rectenna designs is illustrated in Table 3. Hence, the proposed rectenna operates well for all the six resonating frequency bands with higher conversion efficiency. The dimensions of the antenna are also compact compared to existing multiband rectenna designs and it shows circular polarization at three frequency bands as well.

**Table 3**
Comparison of proposed work with other rectenna designs.

| Reference | [6] | [7] | [8] | [9] | [10] | Proposed work |
|---|---|---|---|---|---|---|
| Band | Single band | Dual band | Triple band | Quad band | Quad band | Hexa band |
| Operational frequency (GHz) | 2.45 | 1.8, 2.2 | 0.925, 1.850, 2.150 | 0.9, 1.8, 2.1, 2.4 | 0.9, 1.75, 2.15, 2.45 | 4.75, 5.42, 5.76, 6.4, 6.9, 7.61 |
| Substrate | FR-4 | RT/Duroid 5870 | Rogers 3003 | Rogers R04003 | RF-60A-Taconic, TLP-5-Taconic | FR-4 |
| Dimension (mm × mm × mm) | 35 × 35 × 2.5 | 300 × 380 × 1.6 | 84 × 35 × 1.6 | 145 × 145 × 0.508 | 155 × 155 × 7.835 | 90 × 100 × 1.6 |
| Gain (dBi) | 0.5 | 10.9, 13.3 | 7 | 6 | 6 | 7.3 |
| RF efficiency (%) | 62 | 40 | 40 | 84 | 60 | 84 |
| Diode | Schottky diode SMS7630-079LF | Schottky diode Avago HSMS-2852 | Schottky diode SMS-7630 | Schottky Metelics MSS20-141 | Schottky diode SMS-7630 | Schottky diode HSMS-2820 |

## 4. Conclusion

The paper proposes a multiband rectenna operating for six resonating frequencies in the C-band application range. The sensing antenna design is simple, compact in size and shows circular polarization for three resonating frequency bands. In the proposed rectenna, a voltage doubler rectifier is integrated with microstrip antenna through a matching network for achieving higher conversion efficiency. By means of a matching circuitry, the input impedance of patch antenna and rectifier has been matched. With the increasing demand of Internet of Things (IoT) and Machine to Machine (M2M) devices for automatic operation of devices, the proposed RF energy harvesting system can be a suitable candidate for alleviating the demand for battery reenergizing or replacement.

## Appendix A. Supplementary material

Supplementary data associated with this article can be found, in the online version, at https://doi.org/10.1016/j.aeue.2018.06.020.

## References


[1] Brown WC. The history of power transmission by radio waves. IEEE Trans Microw Theory Tech 1984;32(9):1230–42.
[2] Sudevalayam S, Kulkarni P. Energy harvesting sensor nodes: survey and implications. IEEE Commun Surv Tutorials 2011;13(3):443–61.
[3] Valenta CR, Durgin GD. Harvesting wireless power: survey of energy-harvester conversion efficiency in far-field, wireless power transfer systems. IEEE Microwave Mag 2014;15(4):108–20.
[4] Hagerty JA, Helmbrecht FB, McCalpin WH, Zane R, Popovic ZB. Recycling ambient microwave energy with broad-band rectenna arrays. IEEE Trans Microw Theory Tech 2004;52(3):1014–24.
[5] Ren Y-J, Chang K. 5.8-GHz circularly polarized dual-diode rectenna and rectenna array for microwave power transmission. IEEE Trans Microw Theory Tech 2006;54(4):1495–502.
[6] Chuma EL, Rodríguez LdlT, Iano Y, Roger LLB, Sanchez-Soriano MA. Compact rectenna based on a fractal geometry with a high conversion energy efficiency per area. IET Microwaves, Anten Propag 2018;12(2):173–8.
[7] Sun H, Guo YX, He M, Zhong Z. A dual-band rectenna using broadband Yagi antenna array for ambient RF power harvesting. IEEE Antennas Wirel Propag Lett 2013;12:918–21.
[8] Shen S, Chiu CY, Murch RD. A dual-port triple-band L-probe microstrip patch rectenna for ambient RF energy harvesting. IEEE Antennas Wirel Propag Lett 2017;16:3071–4.
[9] Kuhn V, Lahuec C, Seguin F, Person C. A multi-band stacked RF energy harvester with RF-to-DC efficiency up to 84%. IEEE Trans Microw Theory Tech 2015;63(5):1768–78.
[10] Masotti D, Costanzo A, Prete MD, Rizzoli V. Genetic-based design of a tetra-band high-efficiency radio-frequency energy harvesting system. IET Microwaves Antennas Propag 2013;7(15):1254–63.
[11] Khandelwal MK, Kanaujia BK, Dwari S, Kumar S, Gautam AK. Analysis and design of wide band microstrip-line-fed antenna with defected ground structure for Ku band applications. AEU-Int J Electron Commun 2014;68(10):951–7.
[12] Kumar S, Kanaujia BK, Khandelwal MK, Gautam AK. Single-feed superstrate loaded circularly polarized microstrip antenna for wireless applications. Wireless Pers Commun 2017;92(4):1333–46.
[13] Khandelwal MK, Kanaujia BK, Dwari S, Kumar S, Gautam AK. Analysis and design of dual band compact stacked microstrip patch antenna with defected ground structure for WLAN/WiMax applications. AEU-Int J Electron Commun 2015;69(1):39–47.
[14] Saxena S, Kanaujia BK, Dwari S, Kumar S, Tiwari R. A compact microstrip fed dual polarized multiband antenna for IEEE 802.11 a/b/g/n/ac/ax applications. AEU-Int J Electron Commun 2017;72:95–103.
[15] Li Y, Li W, Mittra R. Miniaturization of ACS-fed dual-band antenna with loaded capacitance terminations for WLAN applications. IEICE Electronics Express 2013;10(15):1–8.
[16] Li Y, Li W, Mittra R. A compact ACS-fed dual-band meandered monopole antenna for WLAN and WiMAX applications. Microwave Opt Technol Lett 2013;55(10):2370–3.
[17] Li Y, Li W, Ye Q. A reconfigurable triple notch band antenna integrated with defected microstrip structure band-stop filter for ultra-wideband cognitive radio applications. Int J Antenn Propag 2013;2013:1–13.
[18] Li Y, Yu W. A miniaturized triple band monopole antenna for WLAN and WiMAX applications. Int J Antenn Propag 2015;2015:1–5.
[19] Li Y, Li W, Yu W. A switchable UWB slot antenna using SIS-HSIR and SIS-SIR for multi-mode wireless communications applications. Appl Comput Electromagnetics Soc J 2012;27(4):340–51.
[20] Xu HX, et al. Analysis and design of two-dimensional resonant-type composite right/left-handed transmission lines with compact gain-enhanced resonant antennas. IEEE Trans Antennas Propag 2013;61(2):735–47.
[21] Xu HX, Wang GM, Qi MQ, Xu ZM. A metamaterial antenna with frequency-scanning omnidirectional radiation patterns. Appl Phys Lett 2012;101:173501.
[22] Xu HX, Wang GM, Qi MQ, Cai T. Compact fractal left-handed structures for improved cross-polarization radiation pattern. IEEE Trans Antennas Propag 2014;62(2):546–54.
[23] Xu HX, Wang GM, Qi MQ, Cai T, Cui TJ. Compact dual-band circular polarizer using twisted Hilbert-shaped chiral metamaterial. Opt Express 2013;21(21):24912–21.
[24] Xu HX, Wang GM, Liang JG, Qi MQ, Gao X. Compact circularly polarized antennas combining meta-surfaces and strong space-filling meta-resonators. IEEE Trans Antennas Propag 2013;61(7):3442–50.